Study of Anisotropic Optical Properties of Poly(arylenephenylene) Thin Films: Dependence on Polymer Backbone

Maria Losurdo,*,† Maria Michela Giangregorio,† Pio Capezzuto,†,‡ Giovanni Bruno,† Francesco Babudri,‡,§ Donato Colangiuli,‡ Gianluca M. Farinola,‡ and Francesco Naso‡,§

Istituto di Metodologie Inorganiche e dei Plasmi, IMIP-CNR, Via Orabona 4, 70126 Bari, Italy; Dipartimento di Chimica, Università di Bari, Via Amendola 173, 70126 Bari, Italy; and Centro CNR/ICCOM, Dipartimento di Chimica, Università di Bari, Via Orabona 4, 70126 Bari, Italy

Received January 22, 2003; Revised Manuscript Received April 23, 2003

ABSTRACT: The correlation between the optical properties and microstructural parameters of different poly(arylenephenylene) thin films, deposited by spin-coating, is investigated by spectroscopic ellipsometry. Conjugated polymer films are found to be anisotropic. They are birefringent, with a higher refractive index in the plane of the film than perpendicular to it. This anisotropy is due to a preferential in-plane orientation of the polymer chains. The dependence of both the in-plane and out-of-plane optical constants of the polymeric thin films and of the fundamental $\pi-\pi^*$ transition on the structure of the chain backbone are studied. The change of the $\pi-\pi^*$ transition energy of the polymers from solution to thin film and its correlation with the molecular structure are investigated as indicative of interchain interactions.

Introduction

In the past two decades, linear π-conjugated systems (LCSs) have acquired a growing importance in many areas of modern chemistry and physics of condensed matter. Conjugated polymers and oligomers represent the best-known LCSs,[1] and they have been demonstrated to be important materials for applications in electronic and photonic devices.[2,3] Owing to their electronic properties, these materials should be able to perform all the functions of the traditional inorganic semiconductors, with the distinctive advantage of their ease of processing.[4] Indeed, they have been employed for fabrication of various semiconductor devices, such as organic light-emitting diodes (OLEDs),[5] polymer-based photovoltaic cells,[6] and organic field effect transistors (FETs).[7] Furthermore, they show great promise as components of plastic lasers[8] and "molecular electronic devices".[9]

A wide range of synthetic methodologies are now available for achieving a great variety of different chemical structures and typologies, offering the possibility of a fine-tuning of the electronic properties of these materials and improving their performances for the applications in electronic devices.[5,10] Therefore, improvement of our understanding of the relationships between structure and electronic properties of conjugated polymers is a goal of pivotal importance for designing new materials suitable for the various applications.

The $\pi-\pi^*$ transition energy (ΔE) and the energy gap value (E_g) are two of the most important parameters that affect the characteristics of OLEDs and second- or third-order nonlinear optic devices.[10]

Moreover, determination of the spectral dependence of the refractive index, quantification of absorption, and determination of microstructural parameters of thin organic semiconductor polymeric layers on planar surfaces are of fundamental interest in technological areas of OLEDs, FETs, and electrochromic devices. For example, the external and internal efficiency of polymeric OLED are connected by the factor $1/(2n)^2$, where n is the refractive index of the active layer, and the angular distribution of the light output depends on $\cos\theta/[n(n^2 - \cos^2\theta)^{1/2}]$, where θ is the angle between emission direction and surface normal.[11]

In the real device configuration, the polymeric film is generally deposited onto an absorbing substrate (or there is a metallic contact) that precludes transmittance measurements to determine the optical response of the polymer. Therefore, optical properties are often measured for the polymer in solution, and they are assumed to be also characteristic of the polymer in the film. Indeed, this assumption neglects effects of the substrate/polymer interactions, interchain interactions, and deposition conditions on the optical response of the polymer in the solid state. In this context, the high thickness resolution, the high sensitivity to microstructural and optical characteristics of thin layers, and the nondestructivity of spectroscopic ellipsometry make this optical technique suitable for studies of thin organic polymeric films. An example of application of spectroscopic ellipsometry to the analysis of organic polymer thin films has been reported by Tammer et al.[12,13] The analysis of the optical functions of conjugates polymeric thin films is complicated by the fact that they have been reported to show anisotropy in optical properties.[14,15]

In this paper we report the results of our studies by variable angle spectroscopic ellipsometry (SE) on the anisotropy in the optical functions of various poly(arylenephenylene) thin films deposited by spin-coating. The polymeric films are found uniaxial anisotropic with the refractive index higher for light polarized with its electric field in the plane of the film than perpendicular to it. This indicates, in agreement with previous data,[16,17] that the polymeric chains lie preferentially in the plane of the film. Indeed, the dependence of the anisotropy,

† IMIP-CNR.
‡ Università di Bari.
§ CNR-ICCOM, Bari.
* Corresponding author: Tel +39 0805443562; Fax +39 0805442024; e-mail cscpml18@area.ba.cnr.it.

10.1021/ma0340816 CCC: $25.00
Published on Web 05/23/2003

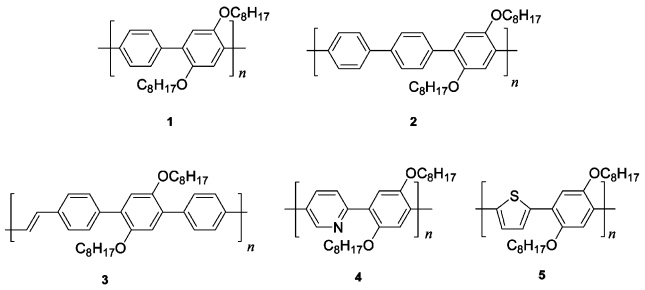

Figure 1. Structures of polymers **1**−**5**.

Scheme 1. General Polymerization Reaction

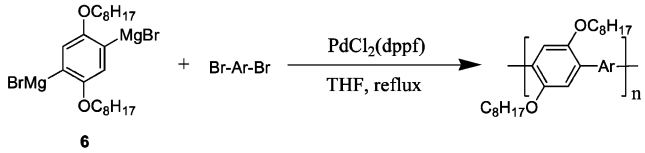

6

Table 1. Polymerization Reactions

polymer	yield[a] (%)	M_n[b,c] (Da)	M_w[c,d] (Da)	M_w/M_n	DP[e]	λ_{max}^{abs}[f] (nm)	λ_{max}^{em}[g] (nm)
1	51	3980	6690	1.68	10	349	417
2	60	8180	11760	1.44	17	350	408
3	58	4150	5910	1.43	8	376	430
4	73	4400	6350	1.45	11	373	428
5	40	4260	7080	1.67	10	466	535

[a] Reaction time 6 days. [b] Number-average molecular mass. [c] Determined by gel permeation chromatography (GPC) with uniform polystyrene standards and THF as a solvent. [d] Weight-average molecular mass. [e] Number-average degree of polymerization. [f] Wavelength of maximum of absorption in chloroform solution. [g] Wavelength of maximum of emission in chloroform solution.

optical functions, and $\pi-\pi^*$ transition of the polymeric thin films on the polymer chain structure is investigated. The focus of the discussion is the comparison of the optical properties of the same polymer in film and diluted solution to highlight the role of the interchain interactions in the solid state on the optical properties.

Experimental Section

Polymer Synthesis and Film Deposition. The synthesis of polymers **1**−**5** (Figure 1) was performed, following a protocol previously developed in our laboratories, by cross-coupling between the Grignard reagent of the 1,4-dibromo-2,5-bis-(octyloxy)benzene (**6**) and the appropriate dihalides in refluxing THF in the presence of dichloro[1,1′-bis(diphenylphosphino)-ferrocene]palladium(II) [$PdCl_2$(dppf)] (Scheme 1) as the catalyst.[18]

The molecular masses of the polymers, together with the values of the wavelengths corresponding to the maximum of absorption and emission in solution, are reported in Table 1.

Determination of Optical Constants. After deposition, the samples were kept under pumping to ultrahigh vacuum to ensure that all solvent was removed. Measuring ellipsometric spectra as a function of time checked stabilization of the polymer films. After stabilization, spectroscopic ellipsometric measurements were performed under vacuum or in a dry N_2 flow to minimize oxygen exposure. Variable angle spectroscopic ellipsometry (SE) spectra of the pseudo-complex refractive index $\langle N \rangle = (n + ik)$ (where n is the real refractive index and k is the extinction coefficient) were measured in the 1.5−5.5 eV energy range at various incidence angles in the range 55°−70° using a phase-modulated ellipsometer (UVISEL, Jobin Yvon). The angle-resolved measurements were useful to check and resolve the anisotropy in the optical properties of thin films according to the approach described in refs 15 and 19. Previous studies[14,15,20] showed that polymeric chains that are approximated by rigid roads lie preferentially in the film plane. This in-plane ordering is difficult to detect by normal and near-normal transmission and/or reflection measurements; hence, reflection at large incidence angles is used to be also sensitive to the in-plane optical constants. Since SE measurements performed rotating the sample in the surface plane around the perpendicular to the film surface were similar, indicating that polymeric chains are randomly oriented in the film plane, a uniaxial model, which distinguishes only between propagation of light parallel to the film surface and perpendicular to it, was used. Consequently, a refractive index in the film plane $(n + ik)_{in-plane}$ and perpendicular to it $(n + ik)_{out-of-plane}$ along the thickness direction were resolved for the anisotropic films of polymers in Figure 1.

To derive the spectral dependence of $(n + ik)_{in-plane}$ and $(n + ik)_{out-of-plane}$ from the measured variable angle SE spectra of the pseudo-refractive index, a simple substrate/film/air model analysis was used. Film thickness was an ellipsometric fitting variable; however, as a starting point of the iterative fitting routine, the film thickness determined independently by stylus profilometry was introduced. SE spectra at all angles of incidence were simultaneously fit to two sets of a double Lorentzian oscillator according to the approach reported in ref 21. This approach is based on the fact that the frequency-dependent dielectric function $\epsilon(\omega)$ of a semiconductor can be expressed by contribution of band-to-band optical transitions that can be taken into account by a combination of Lorentzian oscillators:

$$(n + ik)^2 = \epsilon(\omega) = \epsilon_1(\omega) + i\epsilon_2(\omega) = \epsilon_\infty + \sum_i \frac{f_i {\omega_i}^2}{{\omega_i}^2 - \omega^2 + i\gamma_i\omega} \quad (1)$$

where ϵ_∞ is the high-frequency dielectric constant, ω_i is the resonance frequency, and γ_i is the damping factor of the ith Lorentzian oscillator with strength f_i. With this approach, an oscillator describes the fundamental $\pi-\pi^*$ optical transition whose energy can be precisely determined. The fit quality is evaluated through the unbiased estimator χ^2 defined in ref 22 (the lower the χ^2 value, the better the fit) and the error on each fit parameter and through the correlation matrix of fit parameters. Furthermore, since fitting parameters could be correlated, transmission (T) measurements were also performed to check reliability of extracted optical constants by comparing the ellipsometric derived spectra of the absorption coefficient ($\alpha = 4\pi k/\lambda$) with the absorption spectra (assuming $A = 1 - T$), according to the approach reported in refs 13 and 15.

Results and Discussion

Figure 2 shows a typical example of the SE spectra of the pseudo-refractive index and extinction coefficient acquired at different angles of incidence for the film of polymer **5** and the goodness-of-fit results obtained using the uniaxial anisotropic model.

Both the in-plane and out-of-plane real refractive indexes derived for polymer **5** under the uniaxial anisotropy approximation are shown in Figure 3. In the figure, a comparison of the above data with the refractive index derived using an isotropic model (shown in the same Figure 3) is given.

The isotropic model yields a refractive index that is between the in-plane and out-of-plane refractive indexes obtained assuming anisotropy. Furthermore, the isotropic model required multiple layers of different porosity, resulting anyway in a higher χ^2 value. Note that, by neglecting the anisotropic microstructure, we would observe a different refractive index (see Figure 3) and film porosity or roughness (see that in Figure 3 the isotropic model includes a layer with voids). The incon-

Table 2. Values of Best Fit for the Film Thickness, *d*, the High-Frequency Dielectric Constant, ϵ_∞, the Resonance Frequencies, ω_1 and ω_2, the Oscillator Strength, f_1 and f_2, and Dumping Constant, γ_1 and γ_2, Defined in Eq 1 in the Text for Polymer 5

	d (Å)	ϵ_∞	f_1	ω_1	γ_1	f_2	ω_2	γ_2
$(n,k)_{\text{in plane}}$	1670 ± 26	1.34 ± 0.05	0.47 ± 0.02	2.61 ± 0.01	1.68 ± 0.03	0.89 ± 0.03	7.93 ± 0.17	3.97 ± 0.13
$(n,k)_{\text{out-of-plane}}$		1.40 ± 0.04	2.02 ± 0.12	1.75 ± 0.03	1.52 ± 0.03	0.62 ± 0.03	6.09 ± 0.14	4.06 ± 0.11

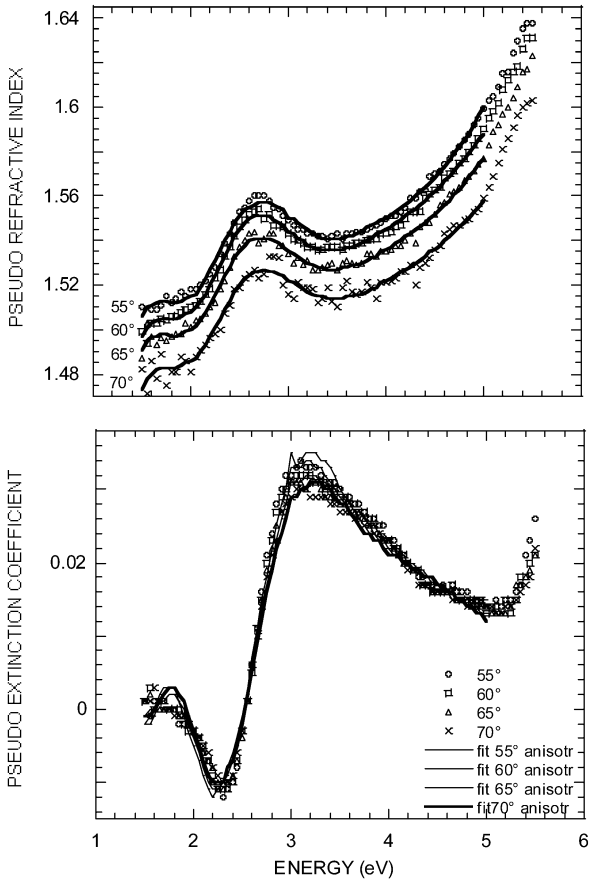

Figure 2. SE spectra at various angles of incidence in the range 55°−70° for polymer **5** of the pseudorefractive index $\langle N \rangle = \langle (n + ik) \rangle$. Symbols are for experimental spectra; lines are for best-fit spectra calculated assuming uniaxial anisotropy.

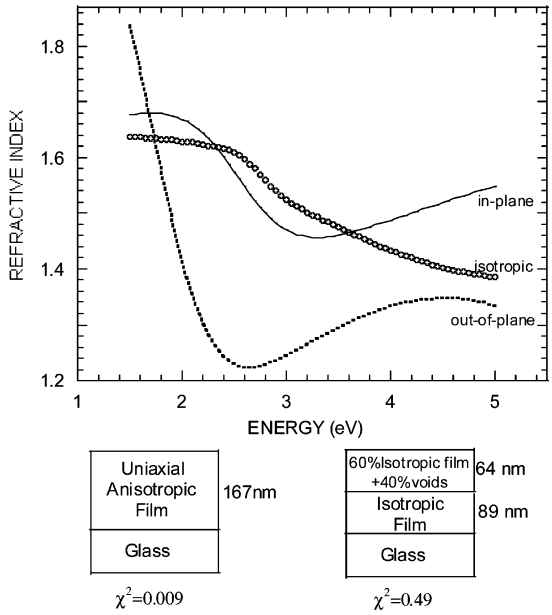

Figure 3. Comparison of the real refractive index for the film of polymer **5** calculated by an isotropic model and an uniaxial anisotropic model both shown at the bottom. In the case of uniaxial anisotropy, both the in-plane and out-of-plane refractive indexes are shown.

sistency of the isotropic model was checked also by AFM measurements that revealed a very smooth surface (a root-mean-square surface roughness; rms = 1 Å was measured for this film).

The above anisotropic values of refractive index result from the fit parameters of eq 1 reported in Table 2 together with the corresponding errors. A film thickness of 1670 Å has been derived by ellipsometry, and this value agrees, within the error, with the value of 170 nm measured by profilometry. Since anisotropic optical constants derived from reflection ellipsometry can be correlated, a way to check the reliability of the extracted data is to consider the correlation coefficients. The correlation matrix for the various fit parameters is reported in Table 3. A correlation coefficient close to 1 or −1 indicates a high correlation between two parameters, i.e., that the fit quality is insensitive to a change in one parameter, since it is compensated by a corresponding change in the other parameter. It can be seen in Table 3 that correlation coefficients are lower than ±0.500, indicating decorrelated fit parameters and, hence, a reliable fit.

Furthermore, transmission measurements that are sensitive to the out-of-plane optical absorption have been used to corroborate the derived $k_{\text{out-of plane}}$ spectra. Figure 4 compares the spectra of the absorption coefficient ($\alpha = 4\pi k/\lambda$ as obtained by the ellipsometric *k* values) and of the absorbance measured for films of polymers **1** and **5**. Good agreement in the energy position of the maximum of absorption and in the spectral shape is found, indicating that SE extracted data are reliable.

The same analysis approach has been applied to films of all the polymers **1**−**5**, and the resulting in-plane and out-of-plane refractive index and extinction coefficient spectra are shown in Figure 5. For all conjugated polymers with exa-atomic rings (i.e., polymers **1**−**4** with the exception of the thiophene-based polymer), a larger dispersion in the refractive index is found for light polarized along the polymer chain, i.e., for the in-plane refractive index. Furthermore, polarized light is more strongly absorbed if the polarization is along the polymer chain. Therefore, the in-plane extinction coefficient is higher than the out-of-plane extinction coefficient, in agreement with data of Chandross et al.[23]

The anisotropic spectra of the extinction coefficient can be used to correlate the degree of optical anisotropy to the degree of chain alignment in the film plane depending on the polymer backbone. According to ref 17, the angular distribution

$$d_{\pi\theta} = \frac{1}{1 + k^{\pi-\pi^*}_{\text{out-of-plane}}/k^{\pi-\pi^*}_{\text{in-plane}}} \qquad (2)$$

provides information on polymer chain orientation (the in-plane and out-of-plane values of the extinction coefficient, *k*, at the energy resonant with the $\pi-\pi^*$ transi-

Table 3. Correlation Coefficients for the Fit Parameters of Eq 1; *d* Is Film Thickness (Polymer 5)

		in-plane							out-of-plane						
	d	ϵ_∞	f_1	ω_1	γ_1	f_2	ω_2	γ_2	ϵ_∞	f_1	ω_1	γ_1	f_2	ω_2	γ_2
d	1	−0.265	0.285	−0.467	0.445	−0.041	0.005	−0.158	−0.317	−0.161	−0.172	0.302	−0.032	0.037	−0.033
ϵ_∞		1	−0.413	0.090	−0484	−0.587	−0.477	0.046	0.189	0.218	0.040	−0.489	−0.099	−0.411	−0.192
f_1			1	−0.513	0.307	−0.091	−0.011	−0.425	−0.465	0.628	−0.149	0.332	−0.442	0.151	−0.314
ω_1				1	−0.217	0.245	0.230	0.318	0.155	−0.313	0.137	−0.099	0.174	0.153	0.320
γ_1					1	0.190	0.124	−0.110	−0.541	−0.202	−0.061	0.640	0.110	0.087	0.135
f_2						1	0.459	0.283	−0.614	−0.180	0.177	0.115	0.715	0.159	0.415
ω_2							1	0.242	0.395	−0.227	0.217	0.146	0.265	0.627	0.430
γ_2								1	0.102	−0.288	0.345	−0.254	0.307	0.076	0.139
ϵ_∞									1	0.221	0.073	−0.537	−0.040	−0.358	−0.146
f_1										1	−0.152	−0.153	−0.179	−0.167	−0.375
ω_1											1	−0.034	0.244	0.131	0.367
γ_1												1	−0.070	0.168	−0.023
f_2													1	−0.090	0.363
ω_2														1	0.265
γ_2															1

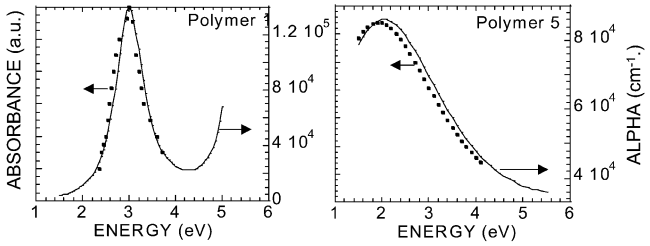

Figure 4. Comparison of the absorption coefficient, α, derived from ellipsometric analysis (continuous line) and of the absorbance (dots) as derived from transmission measurements for polymers **1** and **5**.

tion enter in the eq 2); $k_{out-of-plane}/k_{in-plane} = 1$ and $d_{\pi\theta} = {}^2/_3$ correspond to an isotropic material, while $k_{out-of-plane}/k_{in-plane} \rightarrow 0$ and $d_{\pi\theta} \rightarrow 1$ is the limiting case when chains lay only in the plane. Table 4 summarizes the $d_{\pi\theta}$ values for the various polymers.

For the six-atomic ring values of $d_{\pi\theta}$ in the range 0.844−0.818 are found, similar to the values of 0.91−0.84 reported[17] for highly oriented poly(*p*-phenylenevinylene) (PPV). The obtained values are larger than ${}^2/_3$; hence, it can be inferred that chains lie mainly in the film plane with exception of polymer **5**, where aggregates are supposed to form (see discussion below). Furthermore, the higher $d_{\pi\theta}$ value found for polymer **1** indicates that a backbone with a simple benzene ring results in a preferential chain orientation. The presence of biphenyl ring, double bonds, and heteroatoms in the polymer backbone reduces the preferential orientation and, hence, the anisotropy in the absorption coefficient spectra.

As for the examination of the spectra of the refractive index, it is seen that the polymer backbone strongly affects the energy dispersion of the $n_{in-plane}$, and a higher anisotropy is found again for polymers **1** and **2**. Anisotropy increases with the presence of a biphenyl ring because of the lack of degree of freedom in the chain structure that stiffs the chain in the plane. A backbone with a conjugated double bond results in some flexibility of the polymeric chain and, hence, in a reduced anisotropy in the refractive index.

The SE spectra of the in-plane extinction coefficient in Figure 5 show a dominant peak, which is denoted by the vertical line that results from the fundamental $\pi-\pi^*$ optical transition. The peak of the out-of-plane absorption is slightly blue-shifted from the in-plane feature. According to literature reports,[24] in polymers **1**−**4** the same optical transition is responsible for the peak in both $k_{in-plane}$ and $k_{out-of-plane}$ spectra, and the perpendicular absorption relates to chains that are incompletely aligned. Therefore, the blue shift in the absorption maximum of these chains lying out of the plane of the film is also indicative of a reduction in their effective conjugation length.[15] This reduction is also partially responsible of the $k_{out-of-plane}$ values lower than that of $k_{in-plane}$. Actually, the larger the extent of wave function delocalization, the larger the oscillator strength of the main optical transition.

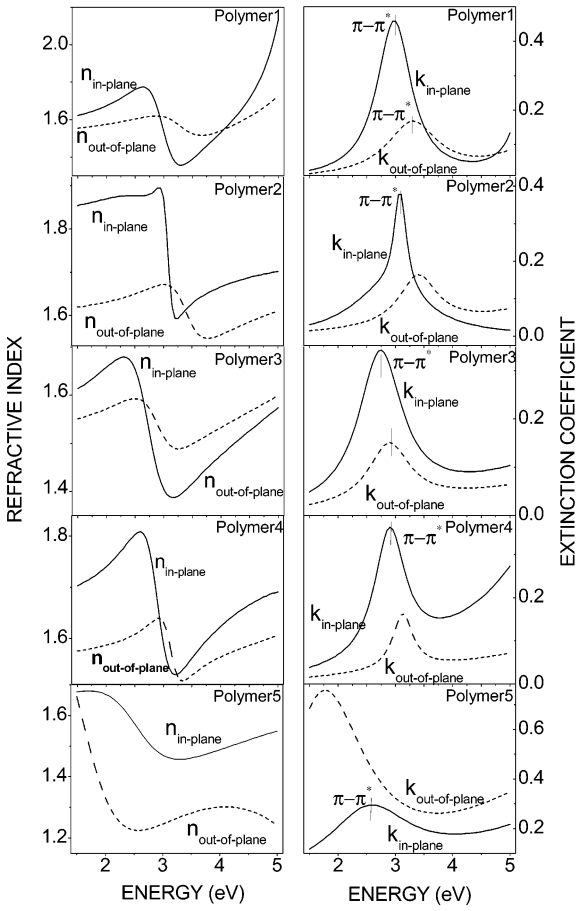

Figure 5. Spectra of both the in-plane and out-of-plane refractive index and extinction coefficient for the films of polymers **1**−**5**.

Table 4. Values of the Angular Distribution $d_{\pi\theta}$ for the Various Polymers of Figure 1

polymer	**1**	**2**	**3**	**4**	**5**
$d_{\pi\theta}$	0.844	0.821	0.819	0.818	0.45

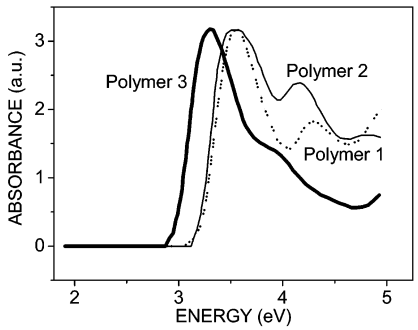

Figure 6. UV−vis spectra of chloroform solutions of the polymers **1**, **2**, and **3**.

Table 5. $\pi-\pi^*$ Transitions of Polymers 1−5 Both in Solution and into Thin Film

polymer	$\pi-\pi^*_{solution}$ (eV)	$\pi-\pi^*_{film}$ (eV)	ΔE (eV)
1	3.56	2.95	−0.61
2	3.55	3.07	−0.48
3	3.30	2.72	−0.62
4	3.33	2.88	−0.35
5	2.66	2.61	0.05

In the case of polymer **5** with the thiophene ring, the in-plane extinction coefficient spectrum shows a peak at 2.61 ± 0.01 eV that agrees with the $\pi-\pi^*$ transition at 2.66 eV measured for the polymer in solution (see below). Hence, this peak is associated with the absorption along polymer chains. However, the in-plane extinction coefficient is lower than the out-of-plane extinction coefficient that has a peak at about 1.72 eV due to a transition polarized primarily perpendicular to the chain axis. A possible explanation for this stronger perpendicular absorption is the formation of particularly stable aggregates in which intermolecular transitions arise due to interactions of π electrons on neighboring chains.[25] Although it is known that oligothiophenes suffer chemical oxidation that can give long-wavelength absorption, here, it is important to underline that the ellipsometric measurements were performed under vacuum (or dry N_2 flux) in order to reduce oxidation of the polymer.

The comparison of the values of the $\pi-\pi^*$ transition energy of the polymers in diluted solutions, i.e., of completely free chains (as determined by means of spectrophotometric UV−vis data and shown in Table 1) with the $\pi-\pi^*$ transition energies of the corresponding films (reported in Table 5) allows to draw some considerations regarding the ΔE values of the various materials and their variation from solution to solid state.

The spectra of chloroform solutions of the polymers **1**, **2**, and **3** are reported in Figure 6. As can be seen, for the two polyphenylene structures (**1** and **2**), the presence of a second nonsubstituted benzene ring in the monomeric unit and the difference of molecular weights (see Table 1) do not affect significantly the $\pi-\pi^*$ transition energy.

Therefore, the effective conjugation length of both materials is quite small. In fact, typical PPPs effective conjugation extension is 9−10 aromatic rings.[26] On the contrary, the further adding of a double bond (polymer **3**) in the monomeric unit, despite the lowest degree of polymerization (DP) (see Table 1), leads to a red shift of the $\pi-\pi^*$ transition of the polymer in solution. This effect is due to the possibility, offered by the double bond, to assume a more planar structure, allowing a greater overlapping of the carbon p_z orbitals and, hence, a more extended electronic density distribution over the polymeric backbone. Moreover, the π-electrons of double bonds are less confined than those of benzene rings;[27] as a result, they can delocalize along the chain more easily, causing an increase in the effective conjugation length.

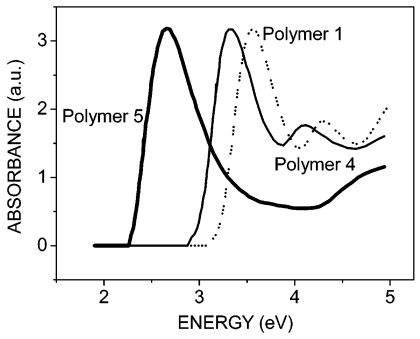

Figure 7. UV−vis spectra of chloroform solutions of the polymers **1**, **4**, and **5**.

The data obtained from the UV−vis spectra of chloroform solutions of polymers **1**, **4**, and **5** (Figure 7) allow to study the effect of the aryl group on the fundamental $\pi-\pi^*$ transition of molecules having the following general structure:

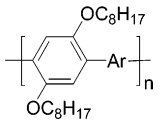

It can be noted that the substitution of the benzene ring with the pyridine and/or thiophene ring is responsible for a red shift of the $\pi-\pi^*$ transition energy due to an increase in extent of conjugation delocalization.

In the film, the trend of ΔE values is the same that in solution, but films are characterized by red shifts of the $\pi-\pi^*$ transition (see Table 5) due presumably to various factors, such as the formation of interchain interactions, the increase in planarization of the polymer backbones, and the in-plane disordered distribution of chains. This is in agreement with the results of Miller et al.,[28] implying that with disorder there is a closer spacing of the delocalized (D) and localized (L) π and π^* bands, i.e., the D−D* and L−D* transitions.

The comparison of the extinction coefficient spectra for films in Figure 5 and the absorbance of solutions highlight the fact that thin films have a nonzero absorption below the fundamental absorption edge that cannot be neglected. From the extinction coefficient spectra (Figure 5), the energy profiles of the absorption coefficient, $\alpha = 4\pi k/\lambda$, have been derived for the in-plane absorption and are shown in the semilogarithmic plot of Figure 8 for the various polymer backbones.

A gradual increase in the absorption extending over several electronvolts is observed below the fundamental absorption edge. This absorption tail is the so-called Urbach's edge[29] which obeys the relationship

$$\alpha(E) = \alpha_0 \exp[(E - E_g)/E_0]$$

where E_0 is the Urbach characteristic energy and E_g is the material band gap. This Urbach region corresponds to electronic transitions between localized defect states in the band-edge tails, the density of which is assumed to fall off exponentially with energy.[30] Hence, E_0 gives

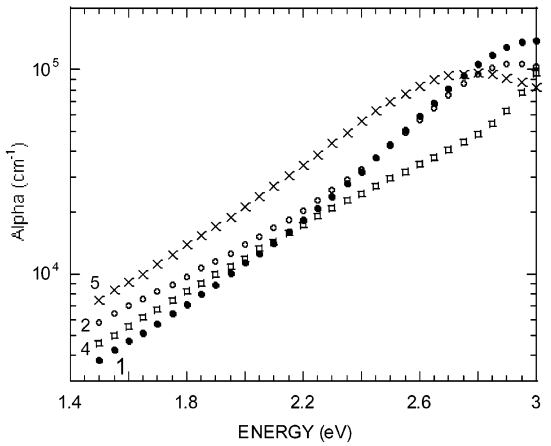

Figure 8. Semilogarithmic plot of the absorption coefficient for films of polymers **1**−**4**.

a measure of the localized defect states originated from microstructural disorder. The derived E_0 values are as follows:

$$E_0 = 0.437\ (\mathbf{1}) < 0.454\ (\mathbf{3}) < 0.526(\mathbf{2}) < 0.549\ (\mathbf{4}) < 0.598\ (\mathbf{5})$$

In particular, the higher E_0 values correspond to a higher absorption in the low-energy tail and are found for films from polymers **5** and **4** characterized by the presence of heterocycles (respectively thiophene and pyridine) in the backbone structure. This indicates that they are more disordered in the plane of the film. The lowest value of E_0 and tail absorption, i.e., the sharpest $\pi-\pi^*$ transition, are found for the simplest polymer **1** with the phenyl ring.

Conclusions

In conclusion, optical functions of conjugated organic polymeric thin films have been determined by variable angle spectroscopic ellipsometry in the range 1.5−5.5 eV. Conjugated polymer films have been found to be anisotropic. In particular, films have been found to be both birefringent, with a higher refractive index in the plane of film than perpendicular to it, and dichroic. This anisotropy is due to a preferential in-plane orientation of the polymer chain. It has been found that the nature of aromatic rings in poly(arylenephenylene)s influences the in-plane preferential orientation and, hence, anisotropy; in particular, from the spectra of the extinction coefficient a preferential in-plane orientation is found for the polymers including in the backbone a simple benzene ring. This result has implications for OLEDs, where the electroluminescence is preferentially emitted perpendicular to the polymer film. The presence of an additional double bond, aromatic ring, or heteroatom decreases the in-plane orientation. In the same manner, the addition of a further benzene ring and of a double bond to a polybiphenylene-based polymer causes an increase of the conjugation effective length in the solid state, affecting the interchain interactions and the $\pi-\pi^*$ transition energy as well as the refractive indexes.

Acknowledgment. The authors thank Ministero dell'Università e delle Ricerca Scientifica e Tecnologica, Rome (Project Sintesi di materiali organici per applicazioni ottiche L.488 19/12/92, Piano "Materiali Innovativi"), for financial support, Prof. E. A. Irene at the Department of Chemistry, North Carolina University, Chapel Hill, NC, for helpful discussion on spectroscopic ellipsometry data and Dr. Michael Stchakovsky at Jobin Yvon, Chilly-Mazarin, France, for some ellipsometric measurements.

References and Notes

(1) *Handbook of Conducting Polymers*; Skotheim, T. A., Elsenbaumer, R. L., Reynolds, J. R., Eds.; Marcel Dekker: New York, 1998.

(2) Bredas, J. L.; Adant, C.; Tackx, P.; Persoons, A. Third-order nonlinear optical response in organic materials: theoretical and experimental aspects. *Chem. Rev.* **1994**, *94*, 243−278.

(3) (a) Müllner, R.; Winkler, B.; Stelzer, F.; Tasch, S.; Hochfilzer, C.; Leising, G. *Synth. Met.* **1999**, *105*, 129−133. (b) *Electronic Materials: The Oligomer Approach*; Müllen, K., Wegner, G., Eds.; Wiley-VCH: Weinheim, 1998.

(4) *Semiconducting Polymers;* Hadziioannou, G., van Hutten, P. F., Eds.; Wiley-VCH: Weinheim, 2000.

(5) Kraft, A.; Grimsdale, A. C.; Holmes, A. B. *Angew. Chem., Int. Ed.* **1998**, *37*, 402−428.

(6) Yu, G.; Gao, J.; Hummelen, J. C.; Wudl, F.; Heeger, A. J. *Science* **1995**, *270*, 1789−1791.

(7) (a) Brown, A. R.; Pomp, A.; Hart, C. M.; de Leeuw, D. M. *Science* **1995**, *270*, 972−974. (b) Garnier, F.; Hajlaoui, R.; Yassar, A.; Srivastava, P. *Science* **1994**, *265*, 1684−1866.

(8) Hide, F.; Diaz-Garcia, M. A.; Schwartz, B. J.; Heeger, A. J. *Acc. Chem. Res.* **1997**, *30*, 430−436.

(9) (a) Seminario, J. M.; Zacarias, A. G.; Tour, J. M. *J. Am. Chem. Soc.* **1999**, *121*, 411−416. (b) Tour, J. M.; Kozaki, M.; Seminario, J. M. *J. Am. Chem. Soc.* **1998**, *120*, 8486−8493.

(10) Roncali, J. *Chem. Rev.* **1997**, *97*, 173−205.

(11) Greenham, N. C.; Friend, R. H.; Bradley, D. D. C. *Adv. Mater.* **1994**, *6*, 491−494.

(12) Tammer, M.; Horsburgh, L.; Monkman, A. P.; Brown, W.; Burrows, H. D. *Adv. Funct. Mater.* **2002**, *12*, 447−454.

(13) Tammer, M.; Monkman, A. P. *Adv. Mater.* **2002**, *14*, 210−212.

(14) Petterson, L. A. A.; Carlsson, F.; Inganas, O.; Arwin, H. *Thin Solid Films* **1998**, *313*−*314*, 356−361.

(15) Ramsdale, C. R.; Greenham, N. C. *Adv. Mater.* **2002**, *14*, 212−214.

(16) Tammer, M.; Higgins, R. W. T.; Monkman, P. *J. Appl. Phys.* **2002**, *91*, 4010−4013.

(17) McBranch, D.; Campbell, I. H.; Smith, D. L.; Ferraris, J. P. *Appl. Phys. Lett.* **1995**, *66*, 1175−1177.

(18) Babudri, F.; Colangiuli, D.; Farinola, G. M.; Naso, F. *Eur. J. Org. Chem.* **2002**, *16*, 2785−2791.

(19) Zangooie, S.; Jansson, R.; Arwin, H. *J. Mater. Res.* **1999**, *14*, 4167−4175.

(20) McBranch, D.; Campbell, H. I.; Smith, D. L.; Ferraris, J. P. *Appl. Phys. Lett.* **1999**, *77*, 1175−1177.

(21) Losurdo, M.; Giangregorio, M. M.; Capezzuto, P.; Bruno, G.; Babudri, F.; Colangiuli, D.; Farinola, G. M.; Naso, F. *Synth. Met.*, in press.

(22) Jellison, G. E. *Thin Solid Films* **1998**, *313*−*314*, 33−39.

(23) Chandross, M.; Mazumdar, S.; Liess, M.; Lane, P. A.; Vardeny, Z. V.; Hamaguchi, M.; Yoshino, K. *Phys. Rev. B* **1997**, *55*, 1486−1491.

(24) Miller, E. K.; Maskel, G. S.; Yang, C. Y.; Heeger, A. J. *Phys. Rev. B* **1999**, *60*, 8028−8033.

(25) Cornil, J.; dos Santos, D. A.; Crispin, X.; Silbey, R. *J. Am. Chem. Soc.* **1998**, *120*, 1289−1293.

(26) Graupner, W.; Grem, G.; Meghdadi, F.; Paar, Ch.; Leising, G.; Scherf, U.; Müllen, K.; Fischer, W.; Stelzer, F. *Mol. Cryst. Liq. Cryst.* **1994**, *256*, 549−554.

(27) Hernandez, V.; Castiglioni, C.; Del Zoppo, M.; Zerbi, G. *Phys. Rev. B* **1994**, *50*, 9815−9823.

(28) Miller, E. K.; Yoshida, D.; Yang, C. Y.; Heeger, A. J. *Phys. Rev. B* **1999**, *59*, 4661−4664.

(29) Urbach, F. *Phys. Rev. B* **1953**, *92*, 1324−1327.

(30) Tauc, J. In *The Optical Properties of Solids*; Abeles, F., Ed.; North-Holland: Amsterdam, 1970; p 277.

MA0340816